from the symmetry axis of the bundle*. Other, more sophisticated fibre geometries would lead to more refined interpretations for δ, but we want to emphasize that the existence of such a δ leading to Equation 2 is independent of the microscopic interpretation we impose upon it.

It should be remarked that recently Scott and Fischbach [4] have discussed an interesting correlation between the total (tensor trace) magnetic susceptibility, χ_T, and the Young's modulus, E, Specifically, they find that there exists a straight line relationship between χ_T and E such that high values of E correspond to large values of χ_T. The quantity $\chi_T = 2|\chi_\perp| + |\chi_\parallel|$ equals 9.3×10^{-6} cm^3 g^{-1} for the composite containing GY-50 and 14.1×10^{-6} cm^3 g^{-1} for that containing GY-70. Since GY-70 has Young's modulus larger than GY-50, the above correlation is confirmed. However, quantitatively our data do not agree with the correlation line (Fig. 1 [4]) proposed by Scott and Fischbach. The reasons for this discrepancy are not clear at the present time.

References

1. W. WATT, *Proc. Roy. Soc. (London)* **A319** (1970) 5.
2. A. R. UBBELOHDE, *Carbon* **14** (1976) 1.
3. S. ARAJS, C. A, MOYER, J. R. KELLY and K. V. RAO, *Phys. Rev.* **B12** (1975) 2747.
4. C. B. SCOTT and D. B. FISCHBACH, *J. Appl. Phys.* **47** (1976) 5329.

Received 30 December 1977
and accepted 25 January 1978.

SIGURDS ARAJS
C. A. MOYER
G. KOTE
Department of Physics,
Clarkson College of Technology,
Potsdam, New York 13676, USA
I. L. KALNINS
Celanese Research Company,
Summit, New Jersey 07901, USA

*It might be argued that $\langle\phi\rangle = 0$ defines the symmetry axis of the bundle, in which case higher order terms in the expression for δ must be retained.

The precracking of fracture toughness specimens of ceramics by a wedge-indention technique

The lack of agreement in the values of fracture toughness obtained by different workers for similar grades of alumina and other ceramic materials is partly due to the absence of a reliable method for precracking the test specimens [1, 2]. A similar problem existed with the determination of fracture toughness values for hardmetals but has recently been solved by the development of a wedge-indentation technique for precracking [3]. Successful use has now been made of wedge indentation to precrack ceramic specimens using alumina and silicon carbide as representative materials.

An indentation technique for precracking ceramics is attractive because it would be simple for small industrial laboratories to use. Pyramid indentation techniques for precracking have been used but they are not widely accepted because of uncertainties about the effect of residual stresses and the geometry of the cracks associated with the indentation. Attempts have been made to remove the stresses by annealing [4] or by grinding [4] away the surface containing the indentation; but annealing could affect the structure and integrity of the material at the crack tip, whilst the small crack size makes it difficult to remove the deformed material completely without removing a substantial part of the crack.

The problems associated with precracking were overcome for hardmetals by using a wedge-shaped indenter (Fig. 1) to produce planar cracks at the midspan position of 4-point bend test specimens. The cracks were much larger than those formed by pyramid indentation and only a small amount of the crack was lost when the plastically deformed zone around the indentation was removed by grinding away the surface with a diamond wheel. It was found that annealing was not a satisfactory way of removing residual stresses associated with the indentation since it produced effects that gave

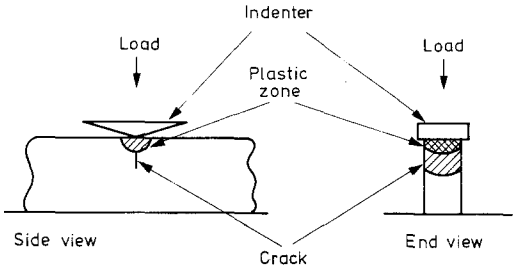

Figure 1 Arrangement of indenter and specimen during precracking by wedge indentation.

too high a value for fracture toughness. The technique proved to be reproducible, simple to use, and did not suffer from the inaccuracies and difficulties of interpretation that are inherent in using the spark machining [5] and pyramid indentation techniques [4].

The wedge indentation technique has now been successfully applied to precrack bend test specimens of a hot-press silicon carbide* and a die-pressed tile of alumina*. Stable crack growth was produced in specimens of both materials by positioning the test pieces on a flat base and loading the wedge indenter at a cross-head speed of 0.005 mm min^{-1} in a 50 kN screw-driven testing machine. Loads of 1 to 2 kN were required and the growth of the cracks to the required depth was followed with a binocular microscope at a magnification of about 20 ×. The wedge indenter was made from polycrystalline diamond and had an included angle of 135°. Fig. 2 shows a side view of cracks produced in bend test specimens of SiC. Just beneath the V-notch produced by the wedge indenter are regions where small petal-shaped slivers of material had flaked away from the test-piece during indentation. The indentation process produced a deformed layer close to the surface and the residual stress field associated with the deformed layer was removed by grinding away the surface layers containing the indentation. The amount of material that had to be removed was determined by measuring the change in the apparent fracture toughness with the depth of material ground from the tensile surface of the test pieces.

Table I shows the results of fracture toughness tests on specimens of SiC and Al_2O_3 tested in a 4-point bend rig with major and minor spans of 29.4 mm and 9.8 mm. Fig. 3 shows the variation of apparent fracture toughness, K, of SiC with the depth of material by grinding after indentation.

The crack length, a, was measured optically both on the side faces of the specimens prior to testing and on the fracture faces of the broken specimens. The crack lengths measured on the fracture surfaces were considered to be more accurate because some difficulty was experienced in locating the exact position of the tip of the crack on the polished side faces. The position of the crack front prior to fracture could easily be seen by dark-field microscopy of the broken specimens because of the slight change in the crack propagation plane which occurred when the test pieces were broken. Fig. 3 shows that it was necessary to remove at least 0.05 mm from the indented surface of the SiC specimen to ensure that a consistent value of fracture toughness was measured.

The average values of fracture toughness for the specimens of SiC and Al_2O_3, where sufficient material was ground away to remove the effects of

TABLE I Fracture toughness tests on SiC and Al_2O_3

Material	Depth of material removed (mm)	Specimen width, B (mm)	Specimen height, W (mm)	a/W	Apparent fracture toughness, K (MN $m^{-3/2}$)
SiC	As-indented	1.83	6.03	0.10	2.7
	0.025	1.83	6.01	0.07	3.3
	0.05	1.84	5.90	0.07	4.8
	0.15	1.84	5.98	0.08	5.2
	0.25	2.72	6.13	0.17	4.8
Al_2O_3	0.20	2.51	4.71	0.17	4.6
	0.20	2.51	4.71	0.13	4.4

*Trade names NC203 and Sintox FA respectively.

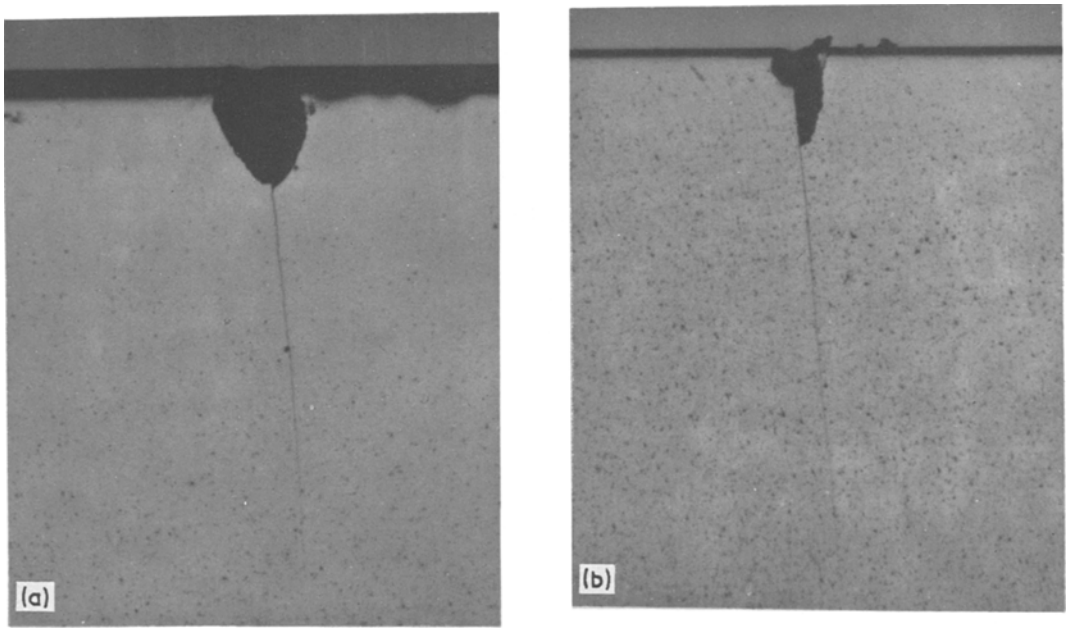

Figure 2 Showing precracks in bend test specimens of silicon carbide.

residual stresses, were 4.9 and 4.5 $MN m^{-3/2}$ respectively, and were reasonable values for the plane strain fracture toughness, K_{IC}. The value of 4.9 $MN m^{-3/2}$ for the fracture toughness of SiC was lower than that obtained from diamond saw-cut notched specimens of the same material [2] where a value of about 6 $MN m^{-3/2}$ had been measured.

Thus the results suggest that it may not be sufficient to notch ceramic specimens in order to obtain valid K_{IC} data, that a true crack is necessary, and that the wedge indentation technique described above is suitable for introducing such a crack into a bend test specimen. The successful use of the wedge indentation technique for precracking hardmetals, with hardness values varying from 1100 HV30 to 1700 HV30, in addition to silicon carbide and alumina, indicates that it could be applicable to a wide range of brittle materials including rocks and glasses as well as other ceramics.

Acknowledgements

Thanks are due to Dr R. Morrell of the Division of

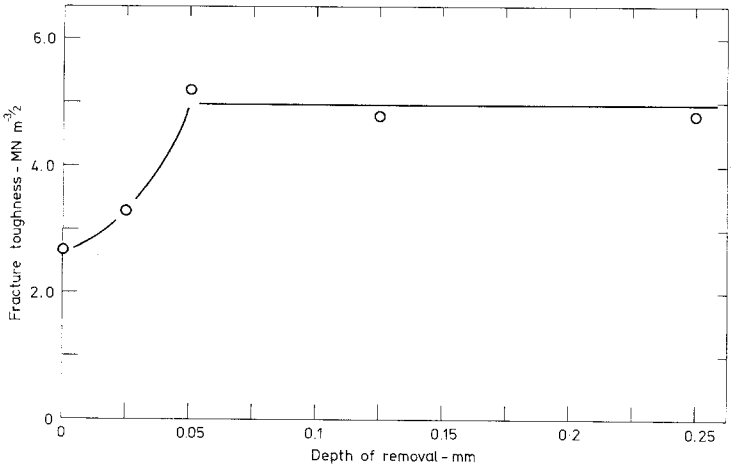

Figure 3 Apparent fracture toughness versus depth of material removed from silicon carbide specimens precracked by wedge indentation.

Chemical Standards, NPL, who provided the sample of alumina and Dr J. L. Henshall of Oxford University who supplied the silicon carbide.

References

1. P. L. PRATT, 4th International Conference on Fracture, *Fracture* 3 (1977) 909.
2. J. L. HENSHALL, D. J. ROWCLIFFE and J. W. EDINGTON, 4th International Conference on Fracture, *Fracture* 3 (1977) 875.
3. E. A. ALMOND and B. ROEBUCK, *Metals Technol.* 5 (1978) 92.
4. J. J. PETROVIC, R. A. DIRKS, L. A. JACOBSON and M. Cr. MENDIRATTA, *J. Amer. Ceram. Soc.* 59 (1975) 177.
5. J. L. CHERMANT and F. J. OSTERSTOCK, *J. Mater. Sci.* 11 (1976) 1939.

Received 3 January
and accepted 31 January 1978.

E. A. ALMOND
B. ROEBUCK
Division of Materials Applications,
National Physical Laboratory,
Teddington, Middlesex, UK

Formation of a DO_{19} phase in zirconium–aluminium martensites

Of the several intermetallic phases that form in the zirconium–aluminium system, the one richest in zirconium occurs around the composition Zr_3Al and has the Ll_2 structure [1, 2]. Recently, Schulson and Graham [3] have examined in detail the formation of this phase in near-stoichiometric alloys through the peritectoid reaction:

$$Zr + Zr_2Al \rightarrow Zr_3Al.$$

It is also possible, in more dilute alloys, to make this phase precipitate in a martensitic or a non-martensitic α-Zr(Al) matrix by ageing in the $\alpha + Zr_3Al$ phase field after quenching from either the beta or the alpha phase regions.

While studying the evolution of Zr_3Al in a martensitic matrix an interesting result was obtained on the basis of certain preliminary observations made on a Zr–4.6 wt % Al alloy and this is briefly reported in this note. The alloy was made in a non-consumable arc furnace in the usual manner, using sponge zirconium and pure (99.99%) aluminium. The finger obtained was homogenized at 1150° C (which corresponded to beta-solutionizing) and was subsequently water quenched to induce the martensitic transformation. Chemical analysis showed that the alloy contained 14 at. % (4.6 wt %) aluminium, 1100 p.p.m. oxygen, 500 p.p.m. carbon and 60 p.p.m. nitrogen.

Transmission electron microscopy revealed that the martensite produced in this alloy was of the dislocated lath type and that the structure appeared to consist of a single phase (Fig. 1). However, selected area diffraction patterns (Fig. 2), obtained from various regions of the samples examined, invariably showed two sets of spots. Those belonging to the first set could be indexed in terms of a disordered hcp structure, having lattice parameters approximately equal to those of alpha zirconium. But the spots of the second set could not be so indexed. These spots, though sharp and well formed, were in general fainter and appeared only at the mid-points of straight lines joining the directly transmitted spot to those spots of the first set that were associated with planes $\{h\,k\,i\,l\}$ for which l was an even integer. The likely reasons for the occurrence of these faint spots could be (i) double diffraction, (ii) an extremely fine scale precipitation of the equilibrium Zr_3Al phase during quenching and (iii) ordering of the α-Zr(Al) solid solution. A systematic examination of the extra spots in various reciprocal lattice sections (obtained from diffraction patterns at various orientations of the foils with respect to the electron beam) showed

Figure 1 Single phase dislocated lath martensite structure of the beta quenched alloys.